Optimal Coordination Control Strategy of Hybrid Energy Storage Systems for Tie-line Smoothing Services in Integrated Community Energy Systems

Dan Wang, *Member, IEEE,* Yunqiang Zhi, Bo Yu, Zhaoyu Chen, Qingsong An, Ling Cheng, and Menghua Fan

***Abstract*—Increasing renewable energy penetration into integrated community energy systems (ICESs) requires more efficient methods to prevent power fluctuations of the tie–line (connection of the ICESs to the main grid). In this paper, centrally-controlled air conditioners are considered as a virtual energy storage system (VESS). The optimal thermostat regulation is used to manage the charging/discharging power of the VESS within the customer comfort level range and the virtual state of charge (VSOC) is used to describe the charging/discharging power of the VESS. On this basis, the model of the hybrid energy storage system is built with a VESS and a battery storage system (BSS). Then, an optimal coordination control strategy (OCCS) for a hybrid energy storage system is developed considering the state-space equation to describe the OCCS, the constraints of the OCCS, and the objective function to express the optimal coordination control performance. Finally, the influence of the outdoor temperature and the deadband of air conditioners on the results of the OCCS is analyzed. Results show that the OCCS can realize optimal allocation of the storage response amount to trace the reference target accurately and guarantee both the state of charge (SOC) of the batteries in a reasonable range to prolong the battery life and ensure the level of comfort experienced by users.**

***Index Terms*—Battery storage system, optimal coordination control, power fluctuation, renewable energy, virtual energy storage system.**

I. Introduction

THE Penetration of renewable energy into integrated community energy systems (ICESs) is on the rise, which leads to power fluctuations and influences the stability and quality of the electricity [1]–[4]. The controllable and schedulable load in ICESs contains various types of thermostatically controlled appliances such as air conditioners, water heaters, and refrigerators. Thermostatically controlled appliances have excellent thermal storage characteristics and can be considered a virtual energy storage system (VESS). They can participate in the energy management of ICESs and be dispatched according to the demand response control strategy. Coordination with typical energy storage systems such as a battery storage system (BSS) can be used to prevent fluctuations induced by renewable energy sources [5]–[7].

Demand response technology can guide users to change their electrical consumption habits. Price signals and incentive policies can change electrical consumption habits of users such that the electrical load over a certain period of time can be transferred or decreased, and an optimal electrical consumption mode can be developed [8], [9]. Demand response technology is used to change the load from residential users or small businesses, typically for the thermal storage capacity of thermostatically controlled appliances such as air conditioners and water heaters [10]–[13]. In addition, it can be extended for central air conditioning systems and appliances in commercial buildings. Through demand response technology, air conditioners can be considered the VESS to participate in energy management to prevent power fluctuations of the tie–line in ICESs and simultaneously guarantee the comfort level of users.

The control strategy to prevent renewable energy fluctuations not only influences the designed amount of batteries and heating/cooling supply appliances in ICESs but also has a great effect on the penetration of renewable energy. Some relevant studies on this subject have been done. An optimal control method of the BSS was proposed in [14] and a tie-line smoothing method that controls the residential heating/cooling supply appliances was proposed in [15]. However, these two methods prevent renewable energy fluctuations only by controlling a single source. In order to comprehensively utilize the source of batteries and the heating/cooling supply appliances in ICESs, a filter algorithm of batteries and the controllable heating/cooling supply appliances was proposed in [16], which can decompose the power fluctuation into high-frequency and low-frequency components and assign them to the heating/cooling supply appliances and batteries, respectively. However, this method can be affected by experience in selecting the filter time constant. Reference [17] proposed a filter algorithm with a variable filter time constant. Reference [18] proposed a battery controlling method based on the state of charge and a variable filter time constant. However, these two methods are

Manuscript received October 11, 2017; revised January 12, 2018; accepted February 12, 2018. Date of publication December 30, 2018; date of current version April 20, 2018. This work was supported by a project of State Grid Corporation of China (No. SGTJDK00KJJS1600035).

D. Wang (corresponding author, e-mail: wangdantjuee@tju.edu.cn), Y. Q. Zhi and Q. S. An are with Tianjin University, Tianjin 300072, China.

B. Yu and Z. Y. Chen are with State Grid Tianjin Electric Power Corporation, Tianjin 300010, China.

L. Cheng is with China Electric Power Research Institute, Beijing, 100192 China.

M. H. Fan is with State Grid Energy Research Institute Co., Ltd, Beijing 102209, China.

DOI: 10.17775/CSEEJPES.2017.01050

2096-0042 © 2017 CSEE

affected by limitations of the filtering algorithm and cannot guarantee the optimal result.

Therefore, an optimal coordination control strategy of hybrid energy storage systems is proposed in this paper, which encompasses the following main contributions:

1) The control strategy takes into account the virtual state of charge (VSOC) that reflects the charge/discharge capabilities of air conditioners as the VESS.

2) The air conditioners considered as the VESS and the BSS are controlled in coordination to prevent power fluctuations of the tie-line in ICESs. Then, an optimal control strategy (OCCS) of hybrid energy storage systems is built.

3) Comparing the control based on the filter algorithm, the proposed optimal coordination control strategy is not affected by human experiences and can accurately follow the smoothing target with continuous constraints of the BSS and the VESS to guarantee the state of charge (SOC) of batteries and the comfort level of users with air conditioners.

4) The influence of the outdoor temperature and the deadband of air conditioners on the results of optimal coordination control strategy are discussed.

This paper is organized as follows: the model of hybrid energy storage systems is presented in Section II, the model of the OCCS is presented in Section III. Results are discussed in Section IV and conclusions are summarized in Section V.

II. Modeling Methodologies of Hybrid Energy Storage Systems

Fig. 1 shows the proposed ICES, which contains renewable energy devices, a BSS, a residential controllable load of air conditioners considered as the VESS, and a residential uncontrollable load. The BSS and the VESS can be flexibly dispatched to satisfy different needs in the ICES. As shown in Fig. 1, measurements from renewable energy sources, the BSS, and the VESS and the uncontrolled loads are sent to a utility management center of the ICES through a two-way communication network. According to different requirements of the management center, the control target signal and the optimal allocation signal for the BSS and the VESS are determined by the optimal control strategy center. By using optimal thermostat regulation (OTR) [12], a centralized load controller located in the optimal control strategy center is used to control the VESS.

With the increasing penetration of renewable energy in the ICES, the power fluctuations of the tie-line need to be restrained. The proposed OCCS consisting of the BSS and the VESS can realize optimal allocation for these energy storage systems to provide the tie-line smoothing services. The power balance formulation as a function of time t is given by:

$$P_{\mathrm{TL}}(t) + P_{\mathrm{RE}}(t) + P_{\mathrm{BT}}(t) = P_{\mathrm{HP}}(t) + P_{\mathrm{NL}}(t) \tag{1}$$

where $P_{\mathrm{TL}}(t)$ is the tie-line power of the ICES, $P_{\mathrm{RE}}(t)$ represents the output of renewable energy, $P_{\mathrm{BT}}(t)$ represents the charge/discharge of the BSS, and $P_{\mathrm{HP}}(t)$ and $P_{\mathrm{NL}}(t)$ respectively represent the consumption of the residential controllable load and the uncontrollable load.

A. Battery Storage Model

In this paper, the kinetic battery model (KiBaM) in [19] is used to describe the battery operation.

The target power P^*_{BT} is determined by the proposed optimal control strategy and the desired discharge current I_{d} is calculated as:

$$I_{\mathrm{d}} = P^*_{\mathrm{BT}}/(N_{\mathrm{s}} V_{\mathrm{rated}}) \tag{2}$$

where N_{s} stands for the number of batteries in the series, and V_{rated} is the rated voltage of each battery.

Suppose that q represents the total current charge, q_1 denotes the amount of charge available, and $q_{1,0}$ and q_0 respectively represent q_1, q at the start-up phase in the current time step. Assuming that $q_1 = 0$ at the end of the time step, the maximum possible discharge current $I_{\mathrm{d,max}}$ is given by:

$$I_{\mathrm{d,max}} = \frac{kq_{1,0}e^{-k\Delta t} + q_0 kc(1 - e^{-k\Delta t})}{1 - e^{-k\Delta t} + c(k\Delta t - 1 + e^{-k\Delta t})} \tag{3}$$

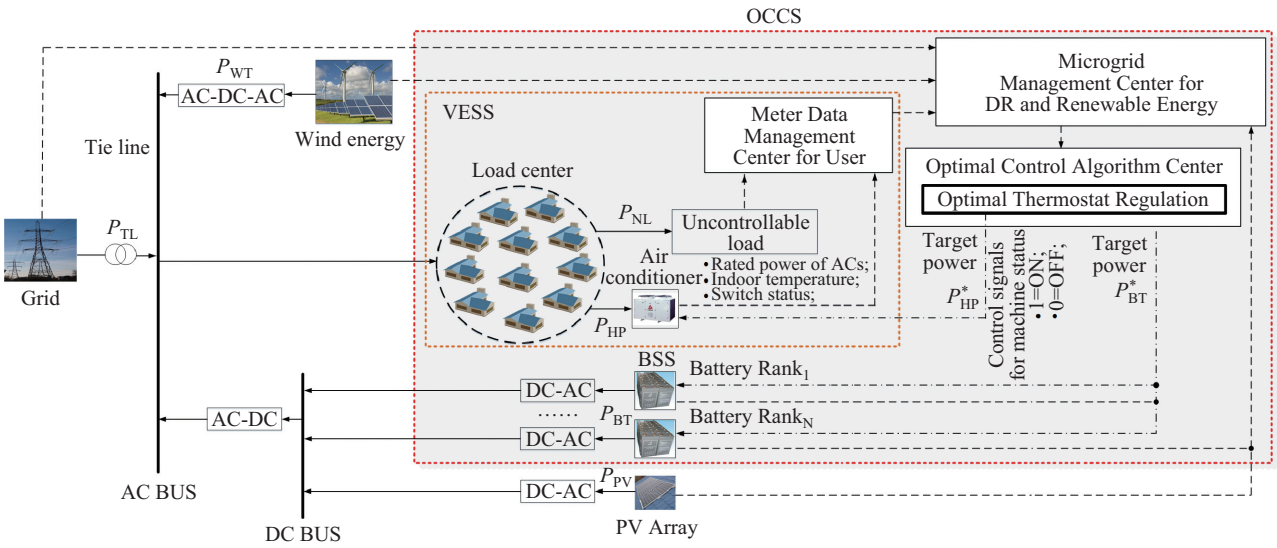


Fig. 1. Configuration of the proposed ICES with a hybrid energy storage system.

where k stands for the ratio constant of the KiBaM, and c denotes the capacity ratio of the KiBaM. If $I_{\rm d} > I_{\rm d,max}$, then $I_{\rm BT} = I_{\rm d,max}$. Otherwise, $I_{\rm BT} = I_{\rm d}$.

Like discharging, the desired charging current is given by:

$$I_{\rm c} = P^*_{\rm BT}/(N_{\rm s}V_{\rm rated}). \tag{4}$$

Assuming $q_1 = cq_{\max}$, the maximum possible charge current $I_{\rm c,max}$ is determined by the following relationship:

$$I_{\rm c,max} = \frac{-kcq_{\max} + kq_{1,0}e^{-k\Delta t} + q_0kc(1-e^{-k\Delta t})}{1-e^{-k\Delta t} + c(k\Delta t - 1 + e^{-k\Delta t})}. \tag{5}$$

If $I_{\rm c} > I_{\rm c,max}$, then $I_{\rm BT} = I_{\rm c,max}$; Otherwise, $I_{\rm BT} = I_{\rm c}$.

In addition, the SOC of the battery banks is described by:

$$\begin{gathered} SOC = q/q_{\max} \\ SOC_{\min} \le SOC \le SOC_{\max} \end{gathered} \tag{6}$$

where $q_{\max}$ describes the maximum capacity of the battery banks, and $SOC_{\max}$ and $SOC_{\min}$ respectively represent the maximum and minimum SOC of the battery banks.

B. Air Conditioner Model

As thermostatically controlled appliances have good controllability, they have become the focus of research in the field of demand response. In this paper, an equal thermal parameter (ETP) model was adapted to describe the thermodynamic behavior of air conditioners [20] as follows:

$$A = \begin{bmatrix} -\left(\dfrac{1}{R_{\rm m}C_{\rm a}} + \dfrac{1}{R_{\rm a}C_{\rm a}}\right) & \dfrac{1}{R_{\rm m}C_{\rm a}} \\ \dfrac{1}{R_{\rm m}C_{\rm m}} & -\dfrac{1}{R_{\rm m}C_{\rm m}} \end{bmatrix}$$

$$B = \begin{bmatrix} \dfrac{1}{R_{\rm a}C_{\rm a}} & \dfrac{1}{C_{\rm a}} \\ 0 & 0 \end{bmatrix},\ T = \begin{bmatrix} T_{\rm a} \\ T_{\rm m} \end{bmatrix},\ C = \begin{bmatrix} T_{\rm o} \\ K \end{bmatrix} \tag{7}$$

$$\dot{\boldsymbol{T}} = \boldsymbol{AT+BC} \tag{8}$$

where $C_{\rm a}$ is the air heat capacity, $C_{\rm m}$ is the mass heat capacity, $R_{\rm a}$ is the air thermal resistant, $R_{\rm m}$ is the mass thermal resistant, T_o is the outside temperature, $T_{\rm a}$ and $T_{\rm m}$ respectively are the inside air and mass temperatures, and K is the electric operation rate.

Equations (7) and (8) can be discretized as a sequence of time steps k separated by time intervals t as:

$$\boldsymbol{T}^k = \boldsymbol{T}^{k-1} + \Delta t(\boldsymbol{AT}^{k-1} + \boldsymbol{BC}^{k-1}). \tag{9}$$

Since the parameters $C_{\rm a}$, $C_{\rm m}$, $R_{\rm a}$, $R_{\rm m}$ change with the customers, a normal distribution function $N(a,\sigma)$ is used to model the load diversity of air conditioner units. The superscripts k and $k-1$ of all variables indicate the values at steps$k$ and $k-1$, respectively.

According to (7)−(9), the temperature and power consumption have a one-to-one relationship. Using the index i to denote the $i^{\rm th}$ air conditioner, the relationship can be described as follows:

$$Q_i^k = Z_i^k \cdot Q_{\rm op} = Z_i^k \cdot \frac{P^i_{\rm rated}}{\eta_{\rm AC}}$$

$$Z_i^k = \begin{cases} 1 & T^{k-1}_{{\rm a},i} \le T^k_{-,i} = T^k_{{\rm s},i} - \dfrac{\delta}{2} \\ 0 & T^{k-1}_{{\rm a},i} \ge T^k_{+,i} = T^k_{{\rm s},i} + \dfrac{\delta}{2} \\ Z_i^{k-1} \end{cases} \tag{10}$$

where $Q_{\rm op}$ is the heat rate, Z_i^k denotes an off/on state of the air conditioner ($Z_i^k = 0$ or 1 for "off" or "on" states, respectively), $T^{k-1}_{{\rm a},i}$ is the current inside temperature, $P^i_{\rm rated}$ is the rated power, δ is the temperature range (deadband), and $T^k_{{\rm s},i}$, $T^k_{+,i}$, $T^k_{-,i}$ respectively represent the temperature set-point and upper and lower temperature limits. Note that (9) actually gives the basic control logic of an air conditioner, i.e., it describes the way the operating status changes.

The operating characteristics of a single air conditioner are shown in Fig. 2, where $\tau_{\rm off}$ and $\tau_{\rm on}$ indicate the time periods when the device is turned on and off, respectively.

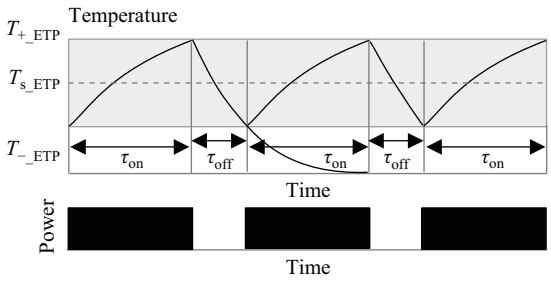


Fig. 2. Operating characteristics of an individual air conditioner.

C. Optimal Thermostat Regulation (OTR) for Aggregated Air Conditioners

As discussed in [13], while considering a large number of air conditioners, a robust control strategy can be applied to regulate the load demand profile by a common perturbation u to the temperature set-point under a centralized control strategy.

For a large number of air conditioners, there is a one-to-one relationship between the temperature and the power consumption, as shown in the discrete histogram displayed in Fig. 3 where the horizontal axis is the temperature and the vertical axis is the power.

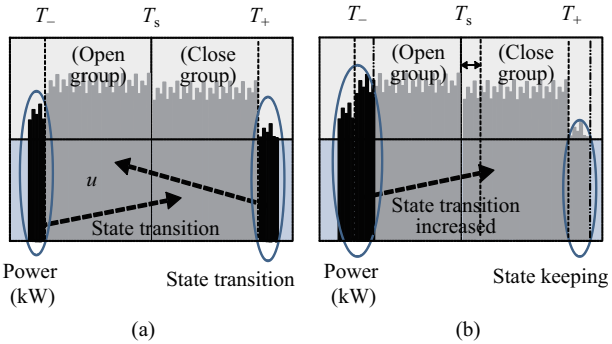


Fig. 3. Discrete temperature-power distribution for uncontrolled mode (a) and controlled mode (b).

To describe the power consumption of a group of air conditioners that have the same temperature state, two temperature-

power factors, ϕ_1^k for "on" states and ϕ_0^k for "off" states, are defined to describe the amount of power at a given air temperature T_{x} as follows:

$$\begin{aligned}\varphi_1^k(T_{\mathrm{x}}) &= \sum_{i=1}^{N} P_{\mathrm{rated}}^i Z_i^k n(T_i^k, T_{\mathrm{x}}) \\ \varphi_0^k(T_{\mathrm{x}}) &= \sum_{i=1}^{N} P_{\mathrm{rated}}^i (1 - Z_i^k) n(T_i^k, T_{\mathrm{x}})\end{aligned} \tag{11}$$

$$Z_i^k = \begin{cases} 1, & (T_{\mathrm{i}}^k \le T_{-,i}^k + T_{\mathrm{u}}^k) \\ 0, & (T_i^k \le T_{+,i}^k + T_{\mathrm{u}}^k) \\ Z_i^{k-1}, & \end{cases} \tag{12}$$

otherwise,

$$n(T_i^k, T_{\mathrm{x}}) = \begin{cases} 1, & (T_i^k = T_{\mathrm{x}}) \\ 0, & (T_i^k \ne T_{\mathrm{x}}) \end{cases} \tag{13}$$

where N is the number of participating air conditioners in the VESS and $n(T_i^k, T_{\mathrm{x}})$ indicates that only devices with temperatures equal to T_{x} play a role in (11).

The total power consumption of the air conditioner population P_{HP}^k at step k can be described as:

$$P_{\mathrm{HP}}^k(T_{\mathrm{u}}^k) = \sum_{T_{\mathrm{x}}=-\infty}^{T_-^k+T_{\mathrm{u}}^k} \varphi_0^k(T_{\mathrm{x}})\Delta\theta + \sum_{T_{\mathrm{x}}=-\infty}^{T_+^k+T_{\mathrm{u}}^k} \varphi_1^k(T_{\mathrm{x}})\Delta\theta \tag{14}$$

where $\Delta\theta$ is the increment of the temperature in the discrete integration represented by (14).

If the target power is known for the next step, the optimal temperature set-point change T_{u} can be obtained by solving the following constrained convex programming problem:

$$\begin{aligned}&\min F = [P_{\mathrm{T}}^k - P_{\mathrm{HP}}^k(T_{\mathrm{u}}^k)]^2 \\ &\text{s.t.}\ \ T_{\min} \le T_-^k + T_{\mathrm{u}}^k < T_+^k + T_{\mathrm{u}}^k \le T_{\max}\end{aligned} \tag{15}$$

where $T_{\max}$ and $T_{\min}$ are the acceptable temperature limits for customers. A method to solve this optimization problem can be found in [21]. In this centralized control strategy, all the air conditioners involved in the calculation are subjected to the same perturbation u.

The air conditioners controlled by OTR can be considered as the VESS. Increasing the number of air conditioners that are turned on is equivalent to charging the VESS and increasing the number of air conditioners that are turned off is equivalent to discharging the VESS.

D. Virtual State of Charge of the VESS

In order to evaluate the charging and discharging ability of the VESS, a VSOC concept was proposed in [16] based on the indoor room temperature of a group of air conditioners. In this paper, the following expression based on power is proposed to calculate the VSOC:

$$\mathrm{VSOC} = \frac{\sum_{i=1}^{N_1} P_{\mathrm{rated}}^i}{\sum_{i=1}^{N_{\mathrm{HP}}} P_{\mathrm{rated}}^i} \tag{16}$$

where N_1 represents the number of air conditioners that are turned on and N_{HP} represents the total number of air conditioners. Considering the comfort requirements of users, the VSOC should be constrained to a specific range that is usually smaller than the entire allowed range from 0 to 1.

III. Modeling Methodologies of Optimal Coordination Control of Hybrid Energy Storage Systems

A. Refrain Target of the OCCS

The tie-line target power $P_{\mathrm{TL}}^{\mathrm{f}}(t)$ can be calculated using a day-ahead prediction without considering the influence of the BSS and the VESS as follows:

$$P_{\mathrm{TL}}^{\mathrm{f}}(t) = P_{\mathrm{HP}}^{\mathrm{f}}(t) + P_{\mathrm{NL}}^{\mathrm{f}}(t) - P_{\mathrm{RE}}^{\mathrm{f}}(t) \tag{17}$$

where $P_{\mathrm{HP}}^{\mathrm{f}}(t)$, $P_{\mathrm{NL}}^{\mathrm{f}}(t)$, $P_{\mathrm{RE}}^{\mathrm{f}}(t)$ represent power prediction values of the controllable load without control, the uncontrollable load, and renewable energy, as shown in Fig. 4. The average of $P_{\mathrm{TL}}^{\mathrm{f}}(t)$ every 60 min gives the tie-line power reference value $P_{\mathrm{TL}}^{\mathrm{ref}}(t)$ shown in Fig. 4(d).

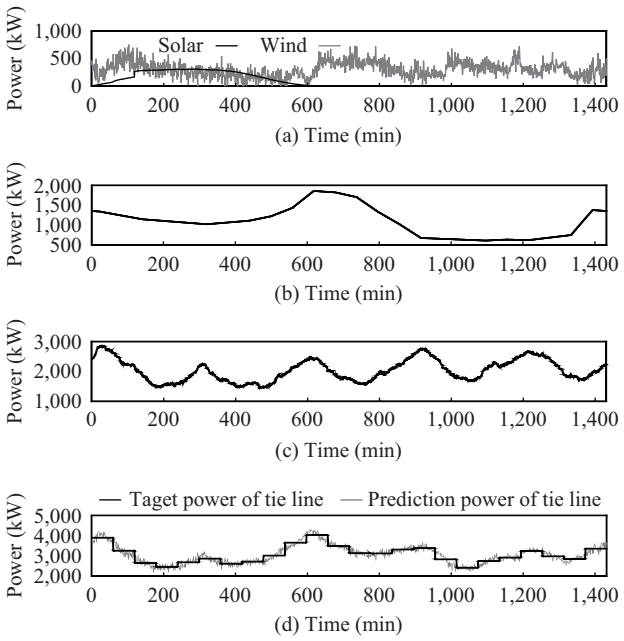


Fig. 4. (a) Power of renewable energy sources. (b) Power consumption of the unresponsive load. (c) Power consumption of the uncontrolled air conditioners. (d) Prediction and reference power of the tie line.

Therefore, the refrain target $y_{\mathrm{ref,t}}$ of the OCCS as a function of time t can be calculated as:

$$y_{\mathrm{ref}}(t) = P_{\mathrm{TL}}^{\mathrm{ref}}(t) + P_{\mathrm{RE}}(t) - P_{\mathrm{NL}}(t) \tag{18}$$

where $P_{\mathrm{RE}}(t)$ is the renewable energy output, $P_{\mathrm{NL}}(t)$ is the consumption of the uncontrollable load, and the actual consumption of the uncontrollable load is assumed to be equal to its prediction value, i.e., $P_{\mathrm{NL}}(t) = P_{\mathrm{NL}}^{\mathrm{f}}(t)$.

B. State Space Equation of the OCCS

The charge of the battery $q(t)$ and the consumption power of the air conditioner group $P_{\mathrm{HP}}(t)$ are defined as state variables

$x_1(t)$ and $x_2(t)$, respectively. In addition, the charging current of the battery $I_{\mathrm{BT}}(t)$ and the variation ratio of the consumption power of the air conditioner group $\dot{P}_{\mathrm{HP}}(t)$ are defined as control variables $u_1(t)$ and$u_2(t)$, respectively. The output variable $y(t)$ is given by:

$$y = P^*_{\mathrm{HP}}(t) - P^*_{\mathrm{BT}}(t) \tag{19}$$

where $P^*_{\mathrm{BT}}(t)$ and $P^*_{\mathrm{HP}}(t)$ are the target powers of the BSS and the VESS, respectively.

Based on [17], the relationship between the charge of the battery and the charging current is given by:

$$I_{\mathrm{BT}}(t) = -\frac{q(t) - q(t-\Delta t)}{\Delta t} = -\frac{x_1(t) - x_1(t-\Delta t)}{\Delta t} = u_1(t) \tag{20}$$

which can also be expressed as $\dot{q}(t) = -I_{\mathrm{BT}}(t)$ or $\dot{x}_1(t) = -u_1(t)$.

The charging power is given by:

$$P_{\mathrm{BT}}(t) = \frac{(q(t-\Delta t) - q(t)) * N_{\mathrm{S}} V_{\mathrm{rated}}}{\Delta t} = I_{\mathrm{BT}}(t) N_{\mathrm{S}} V_{\mathrm{rated}} \tag{21}$$

which can also be expressed as $P_{\mathrm{BT}}(t) = N_{\mathrm{S}} V_{\mathrm{rated}} u_1(t)$.

The variation ratio of the consumption power of the air conditioner group $\dot{P}_{\mathrm{HP}}(t)$ is given by:

$$\dot{P}_{\mathrm{HP}}(t) = \frac{P_{\mathrm{HP}}(t) - P_{\mathrm{HP}}(t-\Delta t)}{\Delta t} = \frac{x_2(t) - x_2(t-\Delta t)}{\Delta t} = u_2(t) \tag{22}$$

which can also be expressed as $\dot{x}_2(t) = u_2(t)$.

Based on its standard form, the state space equation in this paper is given by:

$$\dot{\mathbf{x}} = \begin{bmatrix} 0 & 0 \\ 0 & 0 \end{bmatrix} \mathbf{x} + \begin{bmatrix} -1 & 0 \\ 0 & 1 \end{bmatrix} \mathbf{u} \tag{23}$$

$$\mathbf{y} = \begin{bmatrix} 0 & 1 \end{bmatrix} \mathbf{x} + \begin{bmatrix} -N_{\mathrm{S}} V_{\mathrm{rated}} & 0 \end{bmatrix} \mathbf{u} \tag{24}$$

where

$$\begin{cases} \dot{\mathbf{x}} = \begin{bmatrix} \dot{x}_1(t) & \dot{x}_2(t) \end{bmatrix}^{\mathrm{T}} = \begin{bmatrix} \dot{q}(t) & \dot{P}_{\mathrm{HP}}(t) \end{bmatrix}^{\mathrm{T}} \\ \mathbf{x} = \begin{bmatrix} x_1(t) & x_2(t) \end{bmatrix}^{\mathrm{T}} = \begin{bmatrix} q(t) & P_{\mathrm{HP}}(t) \end{bmatrix}^{\mathrm{T}} \\ \mathbf{u} = \begin{bmatrix} u_1(t) & u_2(t) \end{bmatrix}^{\mathrm{T}} = \begin{bmatrix} I_{\mathrm{BT}}(t) & \dot{P}_{\mathrm{HP}}(t) \end{bmatrix}^{\mathrm{T}} \\ \mathbf{y} = y(t) \end{cases} \tag{25}$$

C. Constraints of the OCCS

1) Constraints of the BSS

The constraints of the BSS are reflected in its SOC and its charging current $I_{\mathrm{BT}}(t)$, which can take values in the following ranges:

$$\mathrm{SOC}_{\min} \le \mathrm{SOC} \le \mathrm{SOC}_{\max} \tag{26}$$

$$-I_{\mathrm{c,max}} \le I_{\mathrm{BT}}(t) \le I_{\mathrm{d,max}} \tag{27}$$

where $I_{\mathrm{c,max}}$ and $I_{\mathrm{d,max}}$ respectively represent the maximum charging and discharging currents, and $\mathrm{SOC}_{\min}$ and $\mathrm{SOC}_{\max}$ respectively represent the minimum and maximum values of the SOC.

The constraints described by optimal control variables are given by:

$$\begin{aligned} \mathrm{SOC}_{\min} N_{\mathrm{s}} q_{\max} \le x_1(t) \le \mathrm{SOC}_{\max} N_{\mathrm{s}} q_{\max} \\ -I_{\mathrm{c,max}} \le u_1(t) \le I_{\mathrm{d,max}}. \end{aligned} \tag{28}$$

2) Constraints of the VESS

The constraints of the VESS are reflected in the consumption power of the air conditioner group and its variation ratio given by:

$$\mathrm{VSOC}_{\min} \le \mathrm{VSOC} \le \mathrm{VSOC}_{\max} \tag{29}$$

$$P_{\mathrm{down}} \le \dot{P}_{\mathrm{HP}}(t) \le P_{\mathrm{up}} \tag{30}$$

where P_{up} and P_{down} respectively are the maximum and minimum variation ratios of the consumption power of the air conditioner group, and $\mathrm{VSOC}_{\min}$ and $\mathrm{VSOC}_{\max}$ represent the minimum and maximum values of the VSOC, respectively.

The constraints described by the optimal control variables are given by:

$$\mathrm{VSOC}_{\min} N_{\mathrm{HP}} P_{\mathrm{rated}} \le x_2(t) \le \mathrm{VSOC}_{\max} N_{\mathrm{HP}} P_{\mathrm{rated}} \tag{31}$$

$$P_{\mathrm{down}} \le u_2(t) \le P_{\mathrm{up}} \tag{32}$$

D. Object Function of the OCCS

The target of the OCCS is to make the actual power of the tie line equal to its reference value and the object function is given by:

$$J = \min \int_0^t \left(y_{\mathrm{ref}}(t) - y(t)\right)^2 dt \tag{33}$$

$$= \min \int_0^t \left[(P^{\mathrm{ref}}_{\mathrm{TL}}(t) + P_{\mathrm{RE}}(t) - P_{\mathrm{NL}}(t)) - \right. \tag{34}$$

$$\left. \left(P^*_{\mathrm{HP}}(t) - P^*_{\mathrm{BT}}(t)\right) \right]^2 dt \tag{35}$$

The optimal control problem for OCCS can be defined as finding an admissible control expression such as:

$$\boldsymbol{u}^* = \begin{bmatrix} u_1^*(t) & u_2^*(t) \end{bmatrix}^{\mathrm{T}} = \begin{bmatrix} I^*_{BT}(t) & \dot{P}^*_{HP}(t) \end{bmatrix}^{\mathrm{T}}, \ t \in [t_0, t_f] \tag{36}$$

which satisfies the physical constraints in such a manner that the cost functional $J(\boldsymbol{u}^*)$ has a minimum value.

In order to describe the error of the tie-line power, the root mean square error (RMSE) is introduced as:

$$RMSE = \sqrt{\frac{1}{n} \sum_{t=1}^{n} \left(P^{\mathrm{ref}}_{\mathrm{TL},t} - P_{\mathrm{TL},t} \right)^2} \tag{37}$$

where $P^{\mathrm{ref}}_{\mathrm{TL},t}$ is the reference power of the tie line at time$t$, $P_{\mathrm{TL},t}$ is the actual power of the tie line at time t, and n is the number of simulation steps.

E. Flow Chat of the OCCS

The proposed optimal control model is the linear least squares model (LLSM) and can therefore be solved by the general commercial optimization software based on the gradient descent method. The simulation steps of the OCCS are as follows:

Step 1: Using (17), calculate the day-ahead prediction of the tie-line power;

Step 2: Obtain the real-time output of renewable energy at time t to calculate the refrain target of the OCCS using (18);

Step 3: Allocatey_{ref}according to (23) and the constraints of the OCCS in (25)−(32), and obtain the controlling target of the OCCS;

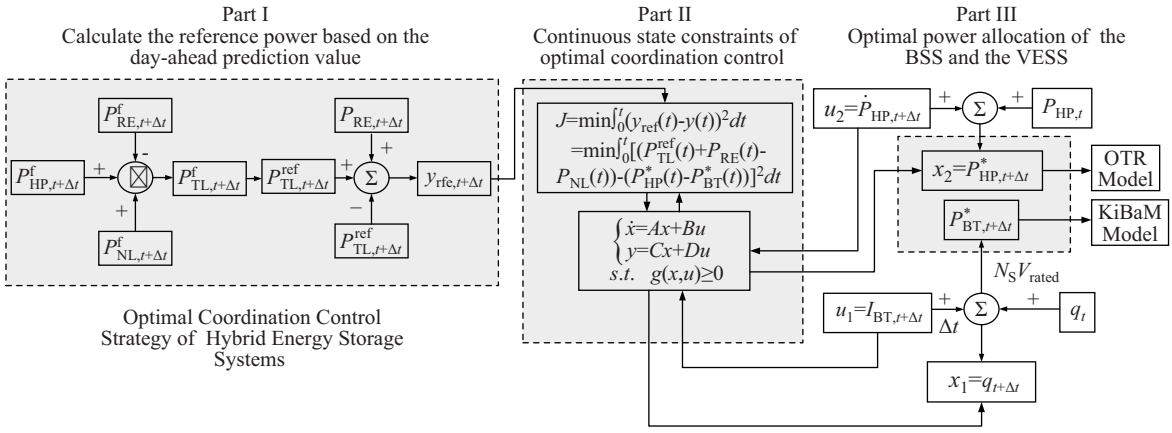


Fig. 5. Flow-chart of the OCCS.

Step 4: Calculate the actual response of the OCCS using (2)−(15);

Step 5: Repeat Step 2 and calculate the optimal control result for the next step until the end of the day.

IV. Simulation and Validation

A. Base Case of the OCCS

In this section, we discuss a case where a total of 1000 air conditioners were set up using the thermal dynamic parameters described in Table I. There were 100 battery banks installed in the ICES and their parameters are listed in Table II. The average outdoor temperature was 5°C and the deadband of the air conditioners was 4°C. The penetration of renewable energy was 10%. The simulation time was 1 day, and the time step was 1 min. The simulation tool MATLAB and the optimal control toolbox TOMLAB were used to realize the algorithm [22].

TABLE I
Parameters of Air Conditioners

Parameter	Symbol	Value
Number of air conditioners	N_{HP}	1,000
Thermodynamic parameters	$\overline{R} = 0.120\ 8^{\mathrm{o}}\mathrm{C/W}$	$\overline{R} = 0.120\ 8^{\mathrm{o}}\mathrm{C/W}$
	$\overline{C} = 3\ 599.3\mathrm{J}/^{o}\mathrm{C}$	$\overline{C} = 3\ 599.3\mathrm{J}/^{o}\mathrm{C}$
	$\overline{Q} = 400\mathrm{W}$	$\overline{Q} = 400\mathrm{W}$
Temperature set-point	T_{set}	21 °C
Temperature deadband	δ	4 °C
Rated power	P_{rated}	6 kW

TABLE II
Parameters of Battery Banks

Parameter	Symbol	Value
Series number	N_{s}	80
Rated terminal voltage	V_{rated}	6 V
Maximum capacity	$q_{\max}$	97.41 Ah
Capacity ratio of KBM	c	0.35
Ratio constant of KBM	K	0.53 hr/s
Time step,	Δt	1 min

From the simulation results in Fig. 6, we can observe the following:

1) As shown in Fig. 6(a), the actual tie-line power can follow its reference power well through the OCCS. However, certain differences exist, particularly around 200−500 min, which are primarily produced in the process of following the target power of the VESS, which occurs because the outdoor temperature at 200−500 minutes is high and the response of air conditioners is slow.

2) As shown in Fig. 6(b) and 6(c), the SOC of the BSS and the VSOC of the VESS are in a reasonable range and the indoor room temperatures for different outdoor temperatures vary within the required range and meet the requirements of users.

3) As shown in Fig. 6(d), the number of on/off transitions of air conditioners under optimal control is more than the number without control, which may have an influence on the service life of air conditioners.

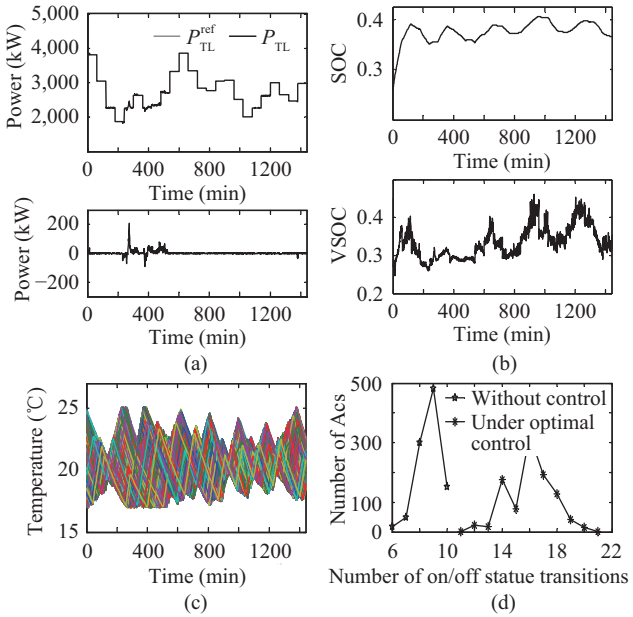


Fig. 6. (a) Reference and actual power of the tie line (top frame) and its error (bottom frame). (b) SOC of the BSS and VSOC of the VESS. (c) Indoor room temperatures. (d) Number of on/off transitions of the air conditioners.

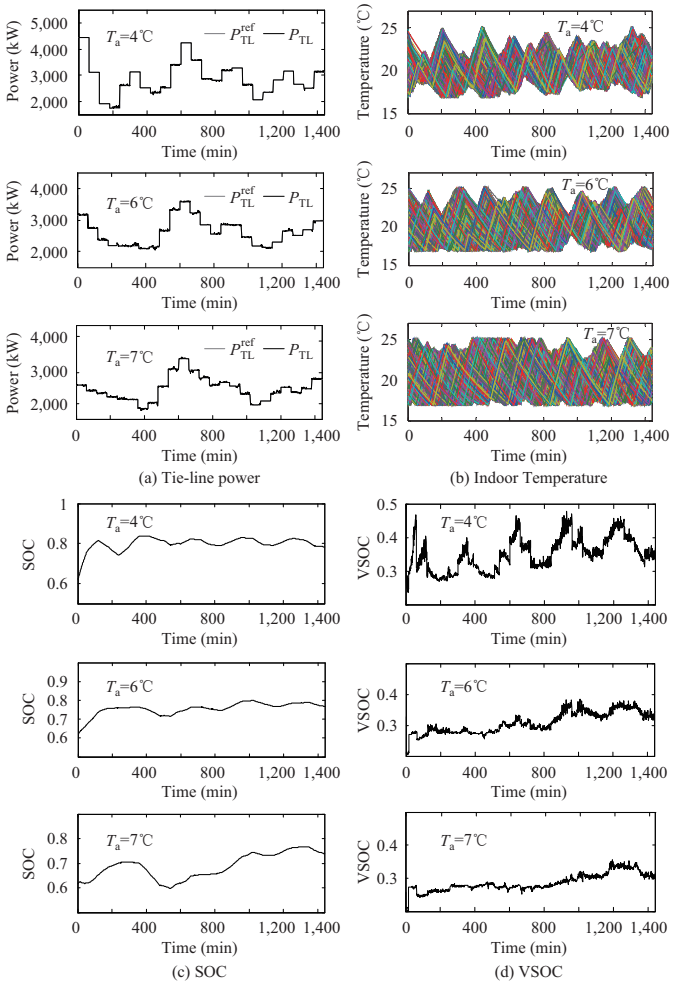


Fig. 7. Results of optimal coordination control for different outdoor temperatures. (a) Tie-line power. (b) Indoor room temperature. (c) SOC of the BSS. (d) VSOC of the VESS.

B. Impact of Outdoor Temperatures on Smoothing Service Quality

In this section, the results of optimal control with different outdoor temperatures of 4°C, 6°C, and 7°C are compared.

From the simulation results in Figs. 7 and 8 and Table III, we can observe the following:

1) As shown in Table III and Figs. 7(a), the OCCS can make the actual tie-line power track its reference power very well under different outdoor temperatures. With rising outdoor temperatures, the RMSE increases because of a decrease in the ability to respond.

TABLE III
RMSEs FOR DIFFERENT OUTDOOR TEMPERATURES

Outdoor Temperature (°C)	RMSE
4	15.53
6	20.30
7	21.59

2) As shown in Figs. 7(b), 7(c), 7(d) and 9, with rising outdoor temperatures, indoor room temperatures fluctuate less frequently and the SOC of the BSS varies in a wider range but the VSOC of the VESS varies in a narrower range and the number of on/off transitions of the air conditioners decreases because of the decrease in the ability to respond.

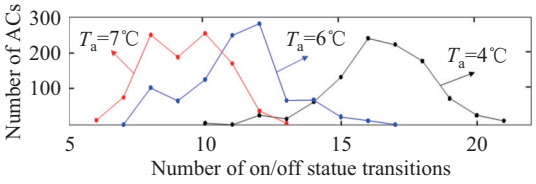


Fig. 8. Number of on/off transitions of the air conditioners for different outdoor temperatures.

C. Impact of Deadband Changes on Smoothing Service Quality

In this section, the results of optimal control with different deadbands of air conditioners are shown. This case compared three different scenarios when the dead-bands of the air conditioners are 2°C, 3°C, 4°C for a 15% penetration of the renewable energy.

From the simulation results in Table IV and Figs. 9 and 10, we can observe the following:

1) As shown in Table IV and Fig. 9(a), when the deadband

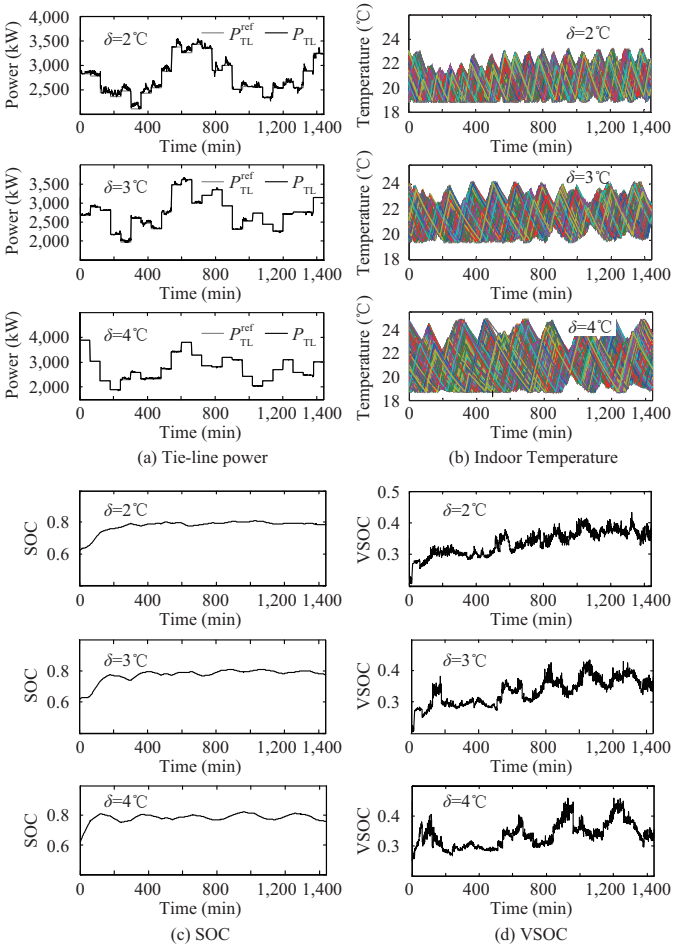


Fig. 9. Results of optimal control for different deadbands. (a) Tie-line power. (b) Indoor temperature. (c) SOC of the BSS. (d) VSOC of the VESS.

of air conditioners decreases, the ability to prevent fluctuations of the tie-line power through the OCCS decreases and the RMSE increases because of the decreased control range of the air conditioners. As shown in Figs. 9(b), 9(c) and 9(d), decreasing the deadband of air conditioners makes the indoor room temperatures fluctuate more frequently while the SOC of the BSS and the VSOC of the VESS are maintained at a higher level.

TABLE IV
RMSEs FOR DIFFERENT DEADBANDS OF AIR CONDITIONERS

Deadband (°C)	RMSE
2	52.34
3	22.67
4	14.07

2) As shown in Fig. 10, the number of on/off transitions of air conditioners increases when the deadband decreases. Since a large number of on/off transitions of air conditioners will damage them, their deadband should not be too small in order to extend their life in practical applications. Therefore, in this scenario, the deadband of 3°C is more preferable.

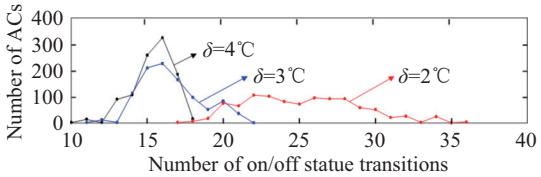


Fig. 10. Number of on/off transitions of the air conditioners for different deadbands.

V. CONCLUSION

In this paper, an optimal coordination control strategy of hybrid energy storage systems based on continuous-state constraints is proposed in ICESs. It is shown that the proposed coordination control strategy could provide an efficient tie-line smoothing service and guarantee the SOC of the BSS and the comfort level of users. Then, numerical studies demonstrate that the different outdoor temperatures have little influence on the smoothing service quality, but the on/off transitions of the air conditioners should be considered in a reasonable range when the outdoor temperature is too low. Finally, different cases demonstrate that the reasonable dead-band of air conditioners is vital for the smoothing service quality and the on/off transitions of the air conditioners. Therefore, the dead-band of air conditioners should be decided considering both the comfort range of users and the simulation results.

REFERENCES

[1] M. Y. Worku, M. A. Abido, and R. Iravani, "Power fluctuation minimization in grid connected photovoltaic using supercapacitor energy storage system," *Journal of Renewable and Sustainable Energy*, vol. 8, no. 1, pp. 439–449, Feb. 2016.

[2] Y. H. Song, Z. F. Tan, H. H. Li, and W. Y. Liu, "An optimization model combining generation side and energy storage system with demand side to promote accommodation of wind power," *Power System Technology*, vol. 38, no. 3, pp. 610–615, Mar. 2014.

[3] J. Hu, S. L. Yang, C. Y. Hou, S. P. Xu, and D. Hui, "Present condition analysis on typical demonstration application of large-scale energy storage technology and its enlightenment," *Power System Technology*, vol. 4, no. 4, pp. 879–885, Apr. 2015.

[4] L. Yang, N. L. Tai, C. J. Fan, and Y. Y. Meng, "Energy regulating and fluctuation stabilizing by air source heat pump and battery energy storage system in microgrid," *Renewable Energy*, vol. 95, pp. 202–212, Sep. 2016.

[5] Q. Zhang, X. R. Li, Y. Ming, Y. J. Cao, and P. Q. Li, "Capacity determination of hybrid energy storage system for smoothing wind power fluctuations with maximum net benefit," *Transactions of China Electrotechnical Society*, vol. 31, no. 14, pp. 40–48, Jul. 2016.

[6] X. K. Xu, M. Bishop, D. G. Oikarinen, and C. Hao, "Application and modeling of battery energy storage in power systems," *CSEE Journal of Power and Energy Systems*, vol. 2, no. 3, pp. 82–90, Sep. 2016.

[7] Q. Y. Jiang and Y. Z. Gong, "Review of wind power integration control with energy storage technology," *Power System Technology*, vol. 39, no. 12, pp. 3360–3368, Dec. 2015.

[8] H. J. Jia, Y. F. Mu, and Y. Qi, "A statistical model to determine the capacity of battery–supercapacitor hybrid energy storage system in autonomous microgrid," *International Journal of Electrical Power & Energy Systems*, vol. 54, pp. 516–524, Jan. 2014.

[9] S. Maharjan, Q. Y. Zhu, Y. Zhang, S. Gjessing, and T. Başar, "Demand response management in the smart grid in a large population regime," *IEEE Transactions on Smart Grid*, vol. 7, no. 1, pp. 189–199, Jan. 2016.

[10] H. J. Jia, Y. Qi, and Y. F. Mu, "Frequency response of autonomous microgrid based on family-friendly controllable loads," *Science China Technological Sciences*, vol. 56, no. 3, pp. 693–702, Mar. 2013.

[11] W. T. Wei, D. Wang, H. J. Jia, C. S. Wang, Y. M. Zhang, and M. H. Fan, "Hierarchical and distributed demand response control strategy for thermostatically controlled appliances in smart grid," *Journal of Modern Power Systems and Clean Energy*, vol. 5, no. 1, pp. 30–42, Jan. 2017.

[12] S. Parkinson, D. Wang, C. Crawford, and N. Djilali, "Comfort-constrained distributed heat pump management," *Energy Procedia*, vol. 12, pp. 849–855, Dec. 2011.

[13] D. Wang, S. Parkinson, W. Miao, H. Jia, C. Crawford, and N. Djilali, "Online voltage security assessment considering comfort-constrained demand response control of distributed heat pump systems," *Applied Energy*, vol. 96, pp. 104–114, Aug. 2012.

[14] S. Teleke, M. E. Baran, S. Bhattacharya, and A. Q. Huang, "Optimal control of battery energy storage for wind farm dispatching," *IEEE Transactions on Energy Conversion*, vol. 25, no. 3, pp. 787–794, Sep. 2010.

[15] C. S. Wang, M. X. Liu, and N. Lu, "A tie-line power smoothing method for microgrid using residential thermostatically-controlled loads," *Proceedings of the CSEE*, vo. 32, no. 25, pp. 36–43, Sep. 2012.

[16] D. Wang, S. Y. Ge, H. J. Jia, C. S. Wang, Y. Zhou, N. Lu, and X. Y. Kong, "A demand response and battery storage coordination algorithm for providing microgrid tie-line smoothing services," *IEEE Transactions on Sustainable Energy*, vol. 5, no. 2, pp. 476–486, Apr. 2014.

[17] R. Wang, D. Wang, H. J. Jia, Z. Y. Yang, Y. B. Qi, M. H. Fan, W. X. Sheng, and L. R. Hou, "A coordination control strategy of battery and virtual energy storage to smooth the micro-grid tie-line power fluctuations," *Proceedings of the CSEE*, vol. 35, no. 20, pp. 5124–5134, Oct. 2015.

[18] Y. Zhang, L. Guo, H. J. Jia, Z. Y. Li, and Z. G. Lu, "An energy storage control method based on state of charge and variable filter time constant," *Automation of Electric Power Systems*, vo. 36, no. 6, pp. 34–38, 62, Mar. 2012.

[19] D. Wang, S. Y. Ge, H. J. Jia, C. S. Wang and N. Lu, "A Demand Response and Battery Storage Coordination Algorithm for Providing Microgrid Tie-Line Smoothing Services," *IEEE Transactions on Sustainable Energy*, vol. 5, no. 2, pp 476-486, Apr. 2014.

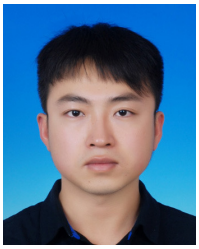
[20] S. Katipamula and N. Lu, "Evaluation of residential HVAC control strategies for demand response programs," *ASHRAE Transactions*, vol. 112, no. 1, pp. 535, Feb. 2006.

[21] N. Lu, "An evaluation of the HVAC load potential for providing load balancing service," *IEEE Transactions on Smart Grid*, vol. 3, no. 3, pp. 1263–1270, Sep. 2012.

[22] Holmström K and Edvall M M, "The TOMLAB Optimization Environment," *Modeling Languages in Mathematical Optimization*. Springer US, vol. 2004, pp. 369–376.



Dan Wang (M'11) received the B.S. and M.S. degrees from Hohai University, Nanjing, China, in 2003 and 2006, respectively, and the Ph.D. degree from Tianjin University, Tianjin, China, in 2009, all in Electric Power Engineering. From 2010 to 2012, he was a Post Doctorate in the Pacific Institute for Climate Solutions, Institute for Integrated Energy Systems, University of Victoria, Victoria, BC, Canada. In 2011, he was a Visiting Researcher in Pacific Northwest National Laboratory, Richland, WA, USA. His current research interests include integrated energy system, distributed generation system, microgrid modeling and simulation, demand-side management, and power system stability analysis.



Yunqiang Zhi received the B.S. degree in Electric Power Engineering from Beijing Institute of Technology, Beijing, China, in 2015. He is now a graduate student in Tianjin University. His research interests include optimization of district integrated energy system and demand-side management.



Bo Yu received the B.S. and M.S. degrees in Electrical Engineering from Tianjin University, China, in 2005 and 2008 respectively, and the Ph.D. degree in Electrical Engineering from Tianjin University, China, in 2012. From 2013 to 2014, he was an Engineer with the State Grid Tianjin Electric Power Corporation. Since 2015, he has been a Senior Engineer with the State Grid Tianjin Electric Power Corporation. His research interests include integrated energy system, optimization of MG and DG.



Zhaoyu Chen received the B.S. and M.S. degrees in Electrical Engineering from Tianjin University, China, in 2013 and 2016. From 2017, he was an Engineer with the State Grid Tianjin Electric Power Corporation.



Qingsong An received the B.S. degree in Thermal Power Engineering from Harbin Engineering University, Harbin, China, in 2001 and the M.S. degree and Ph.D. degree in Engineering Thermophysics from Tianjin University, Tianjin, China, in 2008. From 2008 to 2010, he was a Postdoctoral Fellow in Tsinghua University, Beijing, China. From 2010 to 2015, he was Lecturer with Key Laboratory of Efficient Utilization of Low and Medium Grade Energy (Tianjin University), Ministry of Education, China. Since 2015, he has been an Associate Professor with the Thermal Engineering Department, Tianjin University, Tianjin, China. His research interests include renewable and clean energy systems, thermodynamic analysis, and heat transfer control under extreme condition, refrigerant and heat pump.



Ling Cheng received the M.S. degree in Engineering Thermophysics from North China Electric Power University, Baoding, China, in 2014. He is now a Research Engineer in China Electric Power Research Institute. His research interests include Energy saving and Power Energy Substitution.



Menghua Fan received the B.S. degree and Ph.D. degree in Electrical Engineering from Tianjin University, China, in 2005 and 2011 respectively. Since 2011, she has been a Researcher in State Grid Energy Research Institute (SGERI), China. Currently, she is a Senior Engineer and Director of Reform and Market Research Group of SGERI. Her research interests include power market, integrated energy system, power system stability analysis and demand response.